



**KTH Machine Design**

Airborne Wear Particles Emissions of  
Commercial Disc Brake Materials  
– Disc Brake Test Stand Simulations at Low  
Contact Pressures and Rotors Pre-conditioned  
with Rust

Jens Wahlström, Lars Olander and Ulf Olofsson

Department of Machine Design  
Royal Institute of Technology  
SE-100 44 Stockholm

TRITA – MMK 2008:16  
ISSN 1400-1179  
ISRN/KTH/MMK/R-08/16-SE

# 1 Abstract

Most modern passenger cars have disc brakes on the front wheels, which unlike drum brakes are not sealed off to the ambient air. During braking, there is wear to both the rotor and the pads. This wear process generates particles, which may become airborne. A problem with measuring airborne wear particles in field tests is to distinguish them from the background noise. Therefore, a disc brake laboratory test stand that allows control of the cleanness of the surrounding air is used. With this test stand the number and size of the airborne wear particles from the pad to rotor contact can be measured online. In this technical report the results from two test series is presented. The first series were preformed at three brake cylinder pressure levels (1.2, 1.7 and 2.2 bar) and the rotors were pre-conditioned in a climate chamber with an oxide layer (e.g. rust). Ceramic NAO, NAO and low metallic type brake pads were tested. The second test series were conducted at three low brake cylinder pressure levels (0.1, 0.5 and 1 bar) with NAO and low metallic type brake pads, without any oxide layer. Promising results from the first test series indicate that this test stand can be used to study oxide layer removal from the rotor. The results are also promising for the ability to rank the number and size distribution from different pad rotor material combinations. The second test series shows that even at low pressures measurable levels of airborne particles are generated.

---

Key words: wear, airborne particles, disc brake, oxide layer

---

## 2 Table of content

1	Abstract .....	1
2	Table of content .....	2
3	Introduction .....	3
4	Experimental setup .....	4
5	Test setup .....	5
6	Results .....	7
6.1	First test series - Low metallic type brake pads .....	10
6.2	First test series - NAO type brake pads.....	16
6.3	First test series - Ceramic NAO type brake pads.....	22
6.4	Second test series - Low metallic type brake pads .....	24
6.5	Second test series - NAO type brake pads.....	26
7	Discussion .....	28
8	Conclusions.....	30
9	References .....	31

### 3 Introduction

The relation between adverse health effects and the concentration of airborne particles in the atmosphere are well documented [1–3]. In urban environments, airborne particles can come from different sources, for example, demolition and construction [4], resuspended road dust [5], wheel to rail contact [6, 7], car to road contact [8, 9], and disc brakes [10, 11]. During braking both the rotor and the pads are worn and this wear process generates wear particles, some of which may become airborne. Furthermore, to ensure robust brake performance some brake systems may require the pads to be frequently in low pressure contact with the rotor. This dragging may remove any oxide layer (e.g. rust) from the rotor and keeps the contact surfaces clean. A drawback is the drag torque which may increase the fuel consumption and generates wear particles due to that the pads still are in contact with the rotor after the oxide layer is removed from the rotor. It is therefore wishful to reduce the dragging without affecting the performance of the brakes.

A difficulty with measuring airborne brake particles in field tests is to distinguish them from the background noise. Therefore, it may be preferable to use laboratory test stands that allow controlling of the cleanness of the surrounding air. Although several test stands are available, built to study wear and friction at the pad to rotor interface, few studies [12, 13] have focused on wear particles. Recently, Olofsson et al [14], Olofsson et al [15], and Söderberg et al [16] used a pin-on-disc material test stand with a clean air supply to measure the number and size of airborne wear particles online. Wahlström et al [17] constructed a disc brake assembly test stand at component level where it was possible to control the cleanness of the surroundings and measure the airborne particle concentration online. The purpose of this paper is present two test series conducted in this test stand. The first test series focus on oxide layer removal and the second test series focus on airborne particles generated at low pressure levels.

## 4 Experimental setup

The experimental tests were conducted in a component level test stand [17]. A schematic diagram of the test stand is given in Figure 1. A motor drives (K) the rotor and a pneumatic system (M) is used to apply a controlled braking load. A driving shaft (L) transfers the torque from the motor to the wheel bearing, which in turn rotates the disc. The knuckle is mounted to a suspension device. A sealing chamber (G) seals the brake corner from the surroundings.

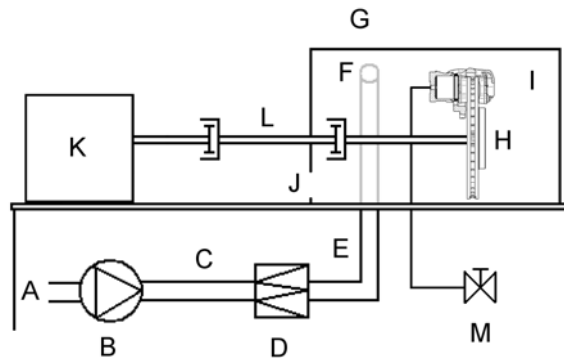


Figure 1. Schematic diagram of the test system. A: room air; B: fan; C: flow rate measurement; D: filter; E: flexible tube; F: inlet for clean air; G: sealing chamber; H: brake corner; I: air inside the chamber, well mixed; J: air outlet, and measurement point for the particle instruments; K: motor; L: driving shaft; and M: pneumatic system.

The applied torque on the motor is measured by a calibrated strain gauge force sensor. The rotational speed of the disc is measured by a built in Hall effect sensor in the wheel bearing. A pneumatic system is used to generate controlled low pressure levels up to 4 bar in the brake cylinder. The pressure level is measured by a calibrated piezoelectric pressure sensor near the inlet of the brake cylinder. The finger side brake pads are prepared with a thermocouple of type K, which measures the temperature near the finger side pad-to-rotor contact. The brake corner, the suspension device for the knuckle, and the driving shaft are contained in the sealing chamber. This chamber is used to control the cleanness of the incoming air. A fan (B) takes the air from the room (A) and presses it into the chamber (G), via a flow measurement system (C) and a filter (D), through the air inlet opening (F). The connections between the fan and the measurement system, between the measurement system and the filter, and between the filter and the chamber are made by flexible tubes (E). In the present test series, all connections from the measurement system to the chamber were sealed to prevent leakages. A leakage could not disturb the tests, since the air pressure inside the tubes was higher than that outside, but a leakage would change the measured air flow rate, which would influence the particle measurements. In the chamber, the air is well mixed (I) due to the complicated volume of the brake corner and the very high air change rate. This is also verified by the

smooth concentrations measured during the tests. The air in the chamber transports the generated particles to the air outlet (J), which is a sample point for the particle measurement. The main particle instrument is an optical particle counter (light scattering) of type Grimm, which measures airborne particles from 0.25  $\mu\text{m}$  to 32  $\mu\text{m}$  in 31 size intervals. The second particle instrument is of type PTrak. This is a condensation nuclei counter that measures the number concentration of airborne particles between 0.02 and 1  $\mu\text{m}$ . The third particle instrument is of type DustTrak, which measures the mass concentration in  $\text{mg}/\text{m}^3$ . This instrument is also of type light scattering and can measure particle concentrations corresponding to respirable size,  $\text{PM}_{10}$ ,  $\text{PM}_{2.5}$  or  $\text{PM}_{1.0}$  size fraction.

## 5 Test setup

Two test series were conducted. In the first series a pair of low metallic, NAO (Non-Asbestos Organic), and Ceramic NAO type of brake pads was combined with a cast iron rotor and tested under stationary load conditions, i.e., constant brake cylinder pressure and rotational speed of the rotor. Pretesting, rotors and brake pads were worn in under stationary cylinder pressure of 1.7 bar and a rotational speed of 600 rpm for 12 minutes. After this running-in period most of the rust protection layer on the rotors was worn off. Thereafter, the rotors was placed in a climate chamber with humid air (80 % atmospheric humidity) for 8 hours to build up an oxide layer (i.e., rust) on the rotors contact surfaces. For each type of brake pads three tests were run at three constant cylinder pressure levels of 1.2, 1.7 and 2.2 bar. The rotational speed was set to 600 rpm in all tests. The first test A started from room temperature; during this test, the oxide layer was worn off. The second test B was conducted directly after the first one without any cooling off period. Thereafter, both pad and rotor were let to cool off to room temperature before a third test C was conducted. Airborne particles were collected on filters during these tests by using pumps. In *Table 1* the test time for each test in the first test series is presented.

*Table 1. Test time [min] for each test run in the first test series.*

	Ceramic NAO			NAO			Low metallic		
[bar]	1.2	1.7	2.2	1.2	1.7	2.2	1.2	1.7	2.2
Test A	-	6	-	6	6	6	6	6	6
Test B	-	6	-	6	6	5	6	6	6
Test C	-	6	-	6	12	6	6	6	6

The second test series were conducted at three low pressure levels of 0.1, 0.5 and 1 bar with NAO and low metallic type brake pads. These tests were conducted without any

oxide layer and started by setting the pressure to 2.5 bar, and directly after decreasing the pressure to the lower level. The rotational speed was set to 600 rpm in all tests and the test time was 12 minutes.

In both test series the fan used to create a constant air flow through the test chamber was set at a flow rate of 33 m<sup>3</sup>/h (9.71 L/s), which gives an approximate air change rate of 144 h<sup>-1</sup> (2.4 min<sup>-1</sup>) during all tests. The air inside the sealed chamber was verified to be particle-free by measuring the particle concentrations in the outlet of the chamber, before the tests started and after the tests were completed. In both cases, the measured particle concentrations were about zero. The measured torque includes the frictional losses in the transmission from the motor to the rotor. To measure this background noise, each test was run for 1 minute with no contact between the pads and rotor before the pneumatic brake load was applied.

While the brake cylinder pressure was applied, the rotational speed of the rotor and brake torque was measured. To keep track of the temperature rise due to the frictional heating at the pad to rotor interface, the NAO and low metallic finger side brake pads was fitted with a thermocouple about 1 mm from the contact surface. During testing the particle concentration was stored every sixth second by the Grimm instrument and every fifth second by the PTrak instrument. The mass concentration was stored every fifth second by the DustTrak instrument. Furthermore, the rotational speed of the rotor, the brake torque and the brake cylinder pressure was measured with a sampling frequency of 1200 Hz. The finger side pad temperature was measured with a sampling rate of 3 Hz.

## 6 Results

The results from the first test series are presented in section 6.1, 6.2 and 6.3 and the second test series in section 6.4 and 6.5. The measured brake torque and finger side pad temperature in the first test series can be seen in Figure 6, Figure 9, Figure 12, Figure 15, Figure 18, Figure 21 and Figure 24 and in the second test series in Figure 27 and Figure 30 . The measured brake torque and the finger side pad temperature for the low metallic type of pads are higher than for the NAO and NAO Ceramic type of pads. Note that the brake torque is corrected for the torque measured with no pressure applied and no contact between the rotor and brake pads. It is also filtered using a 200-point moving average filter. For simplicity, the measured particle concentration is divided into a coarse particle fraction (particles with measured diameters between 1  $\mu\text{m}$  and 32  $\mu\text{m}$ ) and a fine particle fraction (particles with measured diameters lesser than 1  $\mu\text{m}$ ). The measured mass and particle concentration in the first test series can be seen in Figure 4, Figure 7, Figure 10, Figure 13, Figure 16, Figure 19 and Figure 22 and in the second test series in Figure 25 and Figure 28. In the beginning, for all tests A in the first test series, a distinct peak in particle concentration as measured with the Grimm instrument in the coarse fraction can be observed. This peak is up to a factor 5 larger than the number of airborne wear particles generated after this peak. Note that the measured particle concentration by the PTrak is higher than the measure range for the instrument in the first test series for all tests A. The calculated mean particle size distribution during the test time for the first test series is presented in Figure 5, Figure 8, Figure 11, Figure 14, Figure 17, Figure 20 and Figure 23 and for the second test series in Figure 26 and Figure 29. In the first test series, test A\* is the mean particle size concentration taken between 1 and 2.5 minutes and for test A between 2.5 and 7 minutes, and in the second test series test A is the mean particle size distribution over 1 to 7 minutes. The mean particle concentration for test B and C is taken between 1-7 minutes in both test series. Note that all tests have peaks in the mean particle size concentration in the fine fraction around 0.28  $\mu\text{m}$  and 0.35  $\mu\text{m}$  independent of applied brake cylinder pressure and type of brake pad material used and that most of the particles generated are in the fine fraction. In Figure 2 the mean concentration of airborne wear particles generated by the different type of brake pads from the first test series is presented. The mean particle concentrations in the second test series, as measured by the Grimm instrument, are presented in Figure 3.

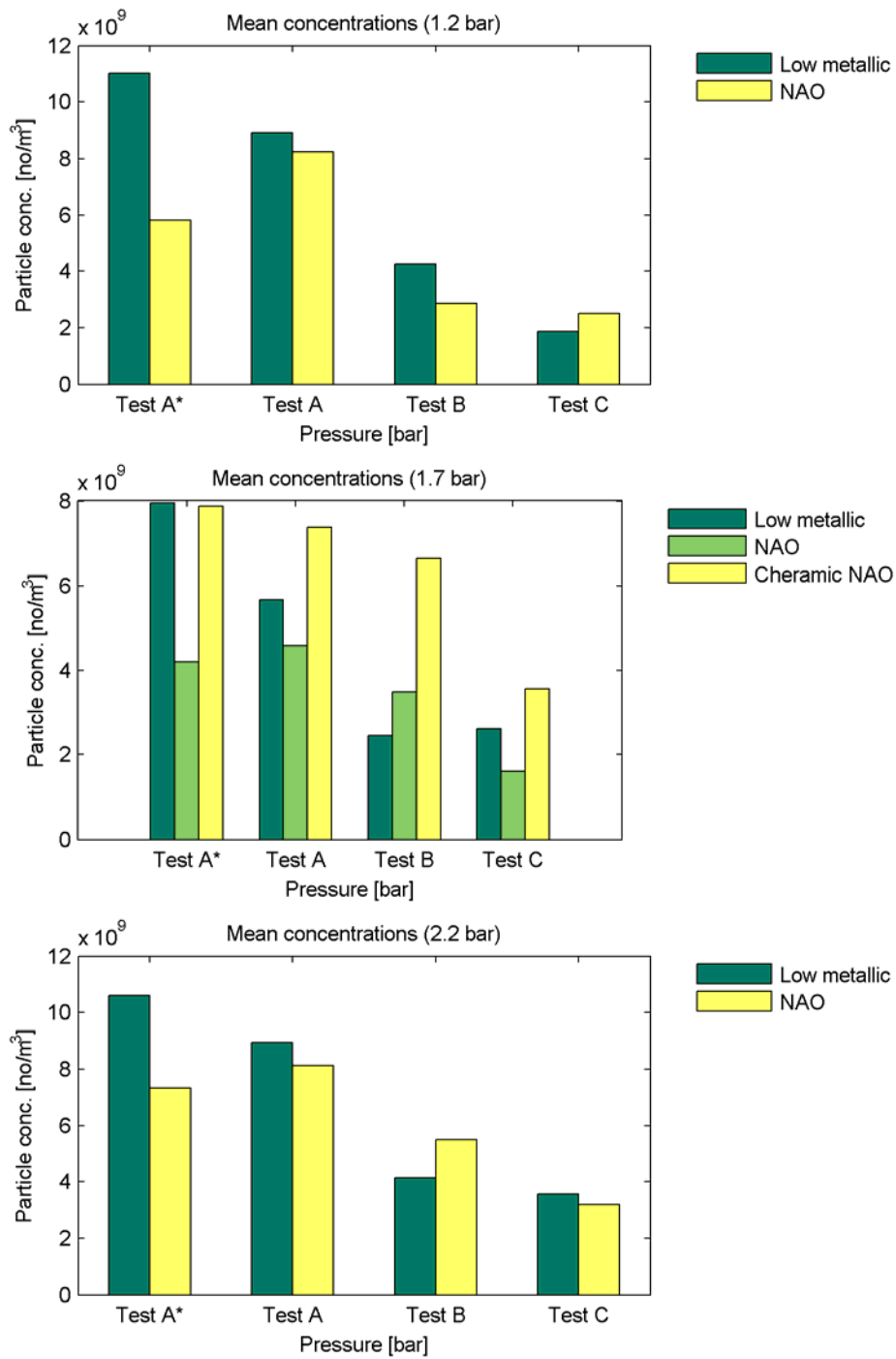


Figure 2. Mean concentrations during test time of airborne particles as measured by the Grimm instrument in the first test series for the low metallic, NAO and ceramic NAO type of brake pads at 1.2, 1.7 and 2.2 bar brake cylinder pressure.

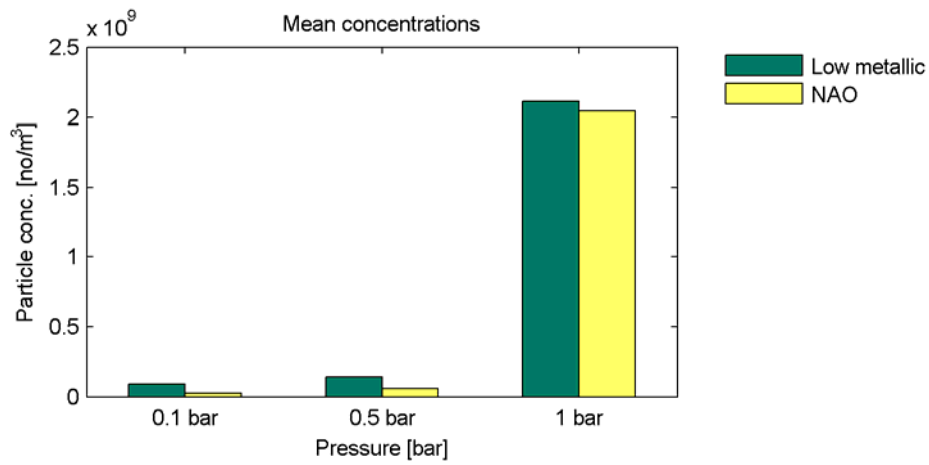


Figure 3. Mean concentrations during test time of airborne particles as measured by the Grimm instrument in the second test series for the low metallic and NAO type of brake pads at 0.1, 0.5 and 1 bar brake cylinder pressure.

## 6.1 First test series - Low metallic type brake pads

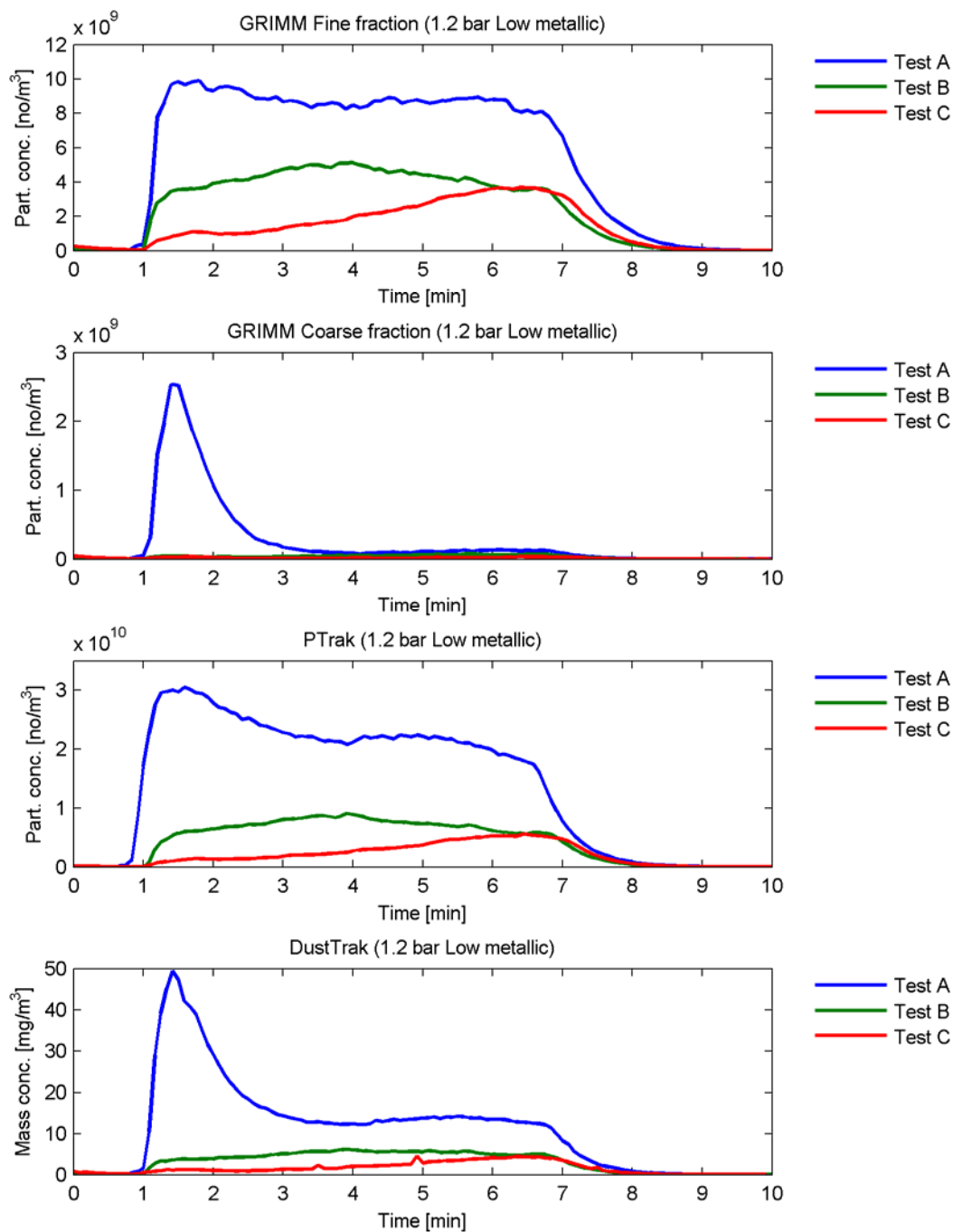


Figure 4. Particle concentrations of airborne wear particles as measured by the GRIMM instrument and the PTrak instrument, and the mass concentration as measured by the DustTrak instrument for the low metallic type brake pads at 1.2 bar.

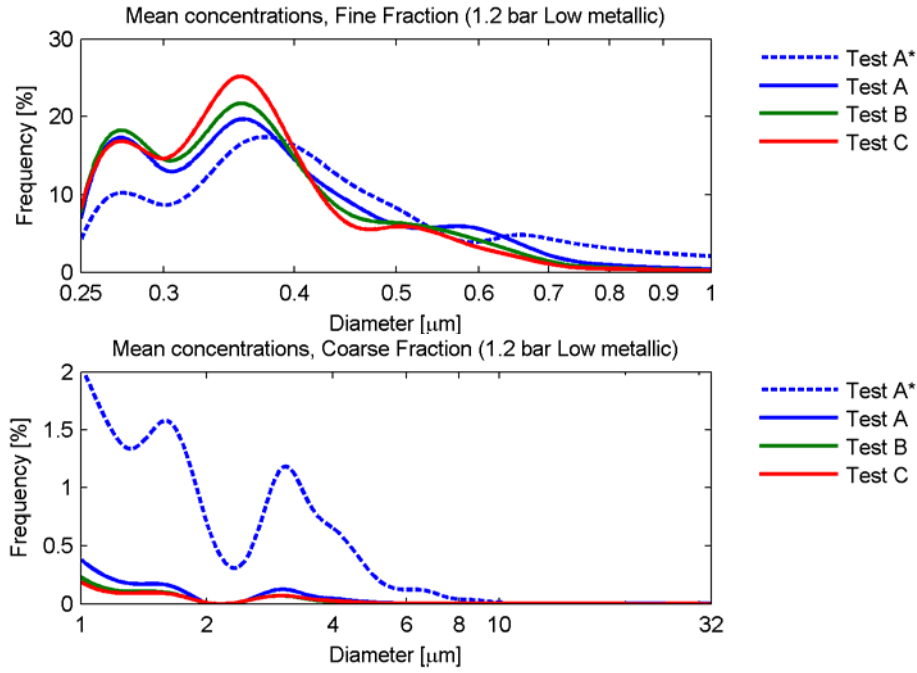


Figure 5. Mean normalized number concentration for the low metallic type brake pads at 1.2 bar as measured with the GRIMM instrument. The mean is taken between 1-2.5 min and 2.5-7 min for test A\* and test A, respectively. For test B and C the mean is taken between 1-7 min.

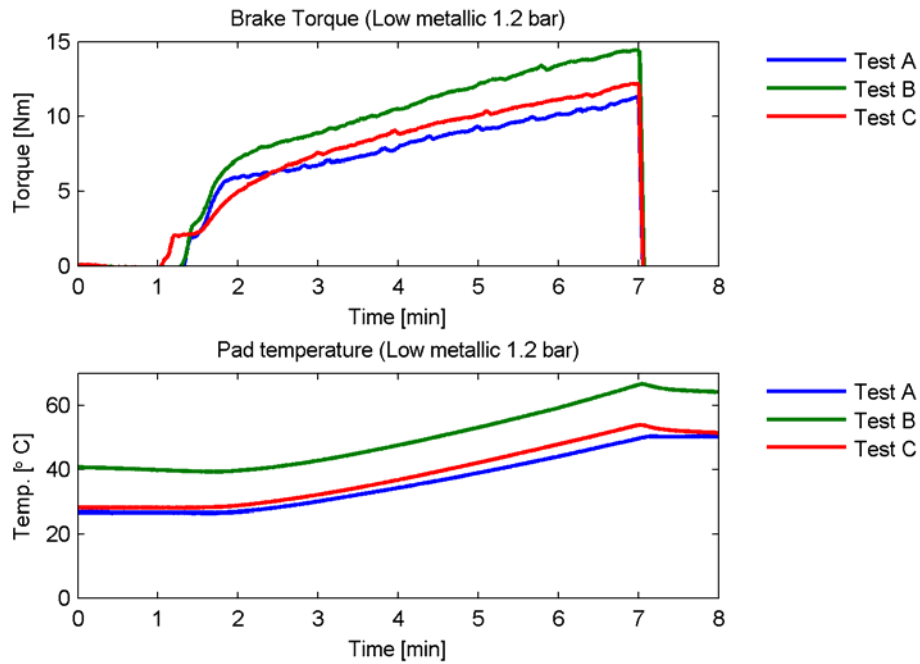


Figure 6. Brake torque and finger side pad temperature during test time for the low metallic type brake pads at 1.2 bar.

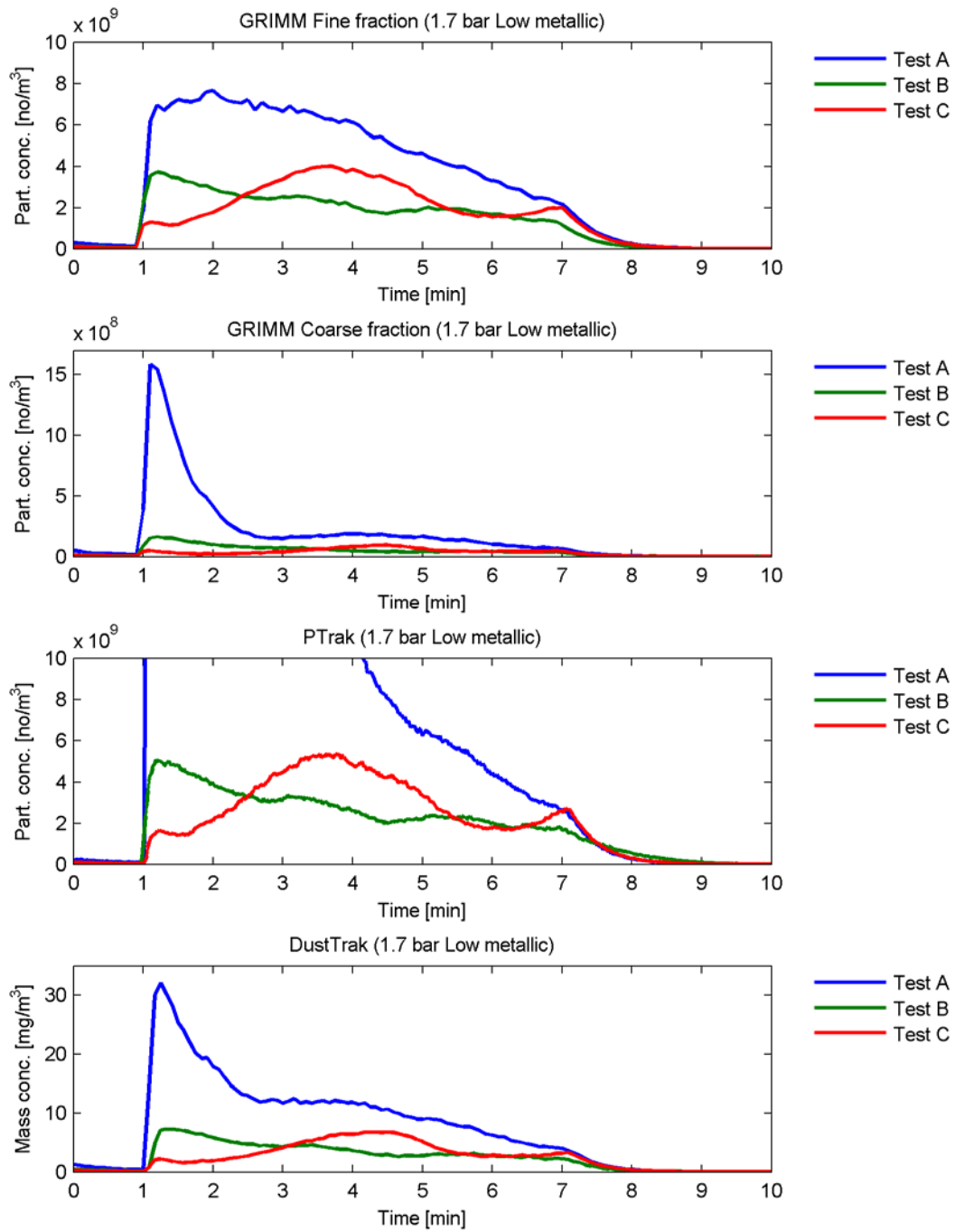


Figure 7. Particle concentrations of airborne wear particles as measured by the GRIMM instrument and the PTrak instrument, and the mass concentration as measured by the DustTrak instrument for the low metallic type brake pads at 1.7 bar.

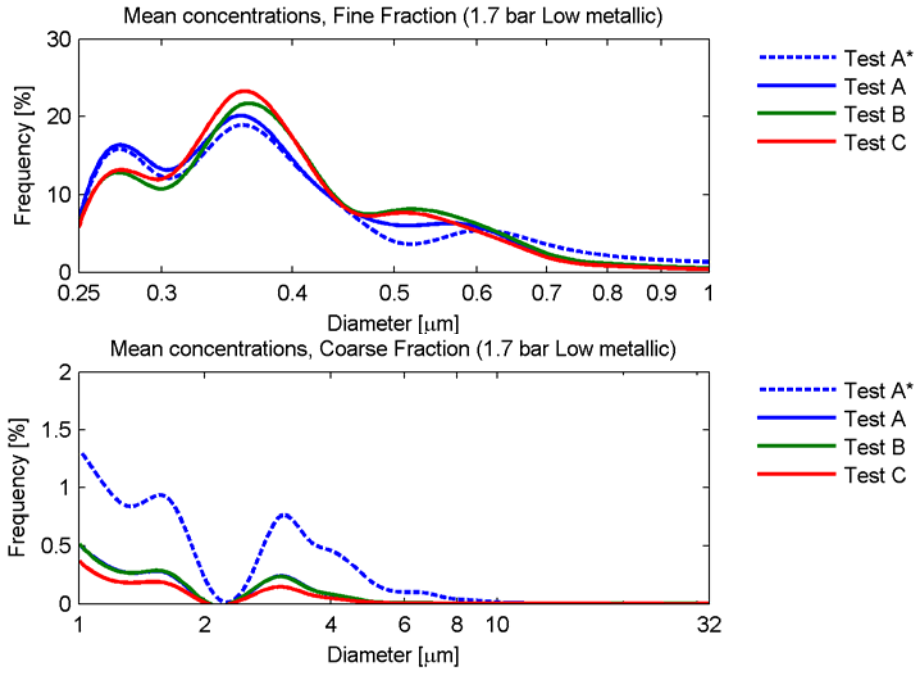


Figure 8. Mean normalized number concentration for the low metallic type brake pads at 1.7 bar as measured with the GRIMM instrument. The mean is taken between 1-2.5 min and 2.5-7 min for test A\* and test A, respectively. For test B and C the mean is taken between 1-7 min.

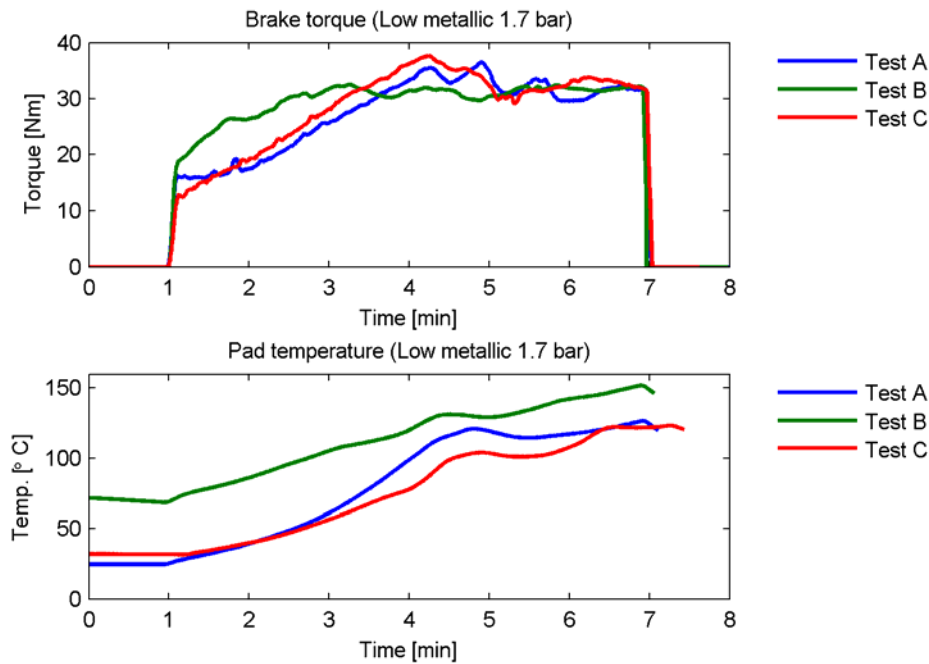


Figure 9. Brake torque and finger side pad temperature during test time for the low metallic type brake pads at 1.7 bar.

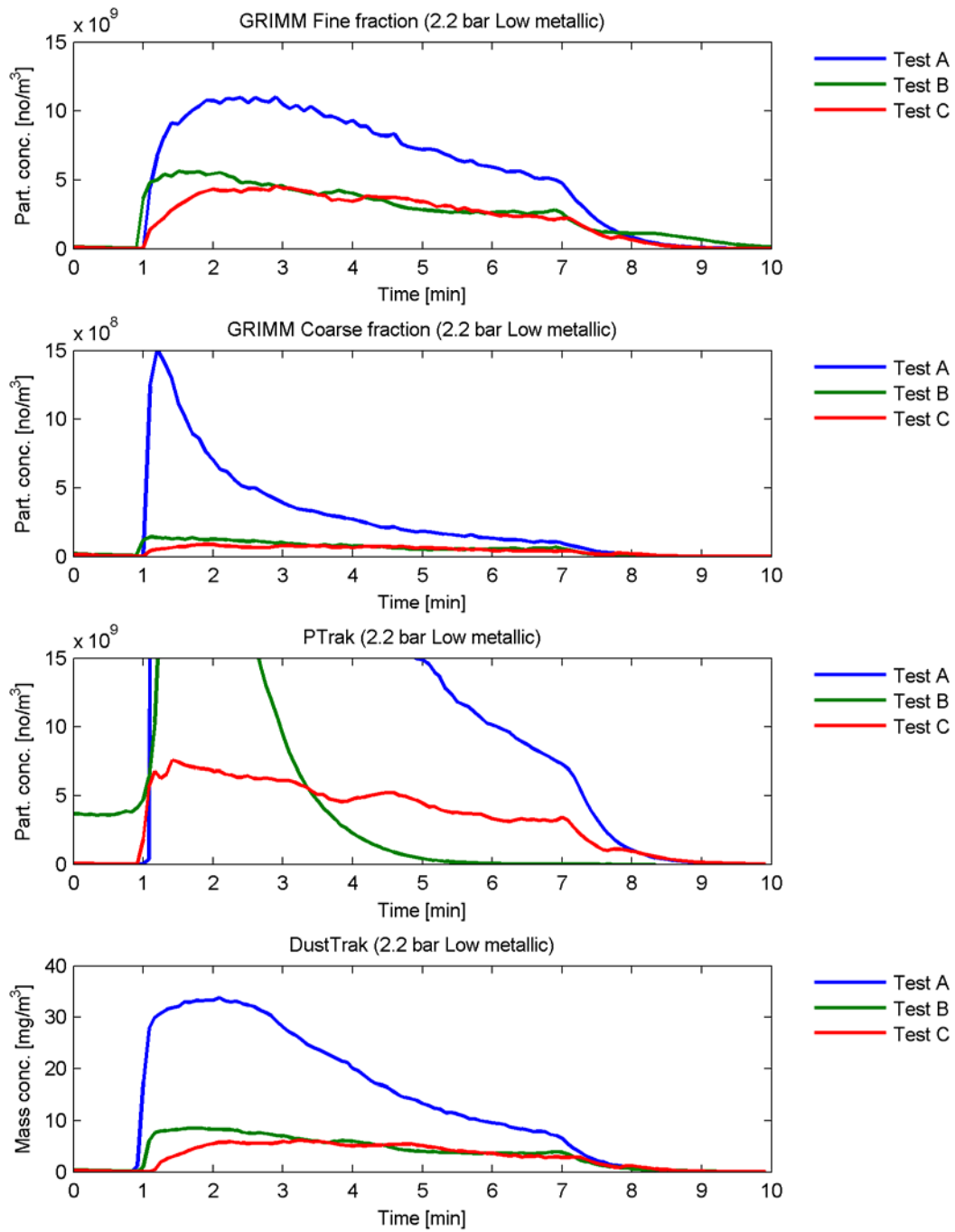


Figure 10. Particle concentrations of airborne wear particles as measured by the GRIMM instrument and the PTrak instrument, and the mass concentration as measured by the DustTrak instrument for the low metallic type brake pads at 2.2 bar.

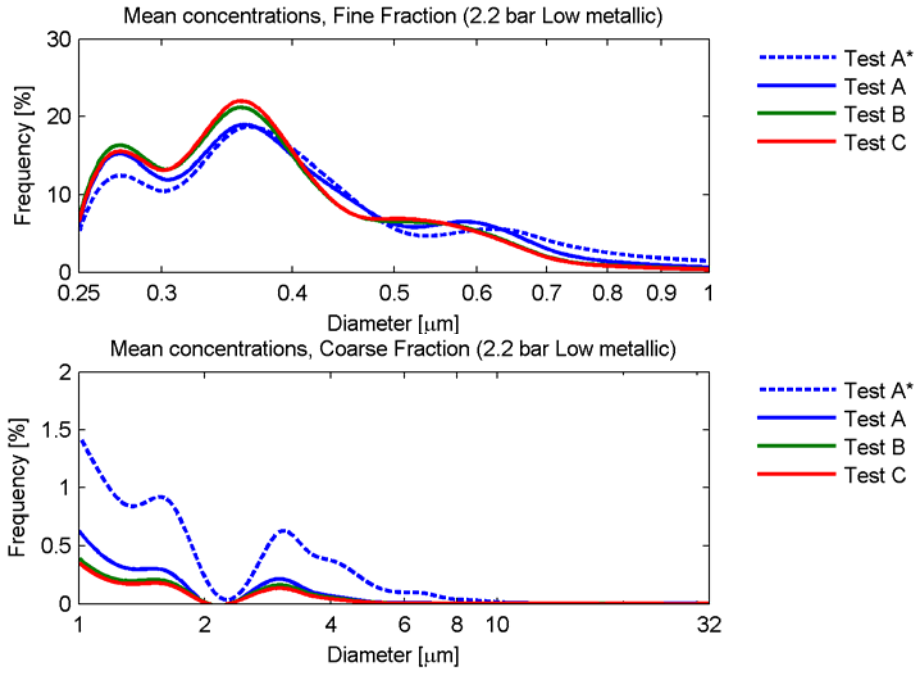


Figure 11. Mean normalized number concentration for the low metallic type brake pads at 2.2 bar as measured with the GRIMM instrument. The mean is taken between 1-2.5 min and 2.5-7 min for test A\* and test A, respectively. For test B and C the mean is taken between 1-7 min.

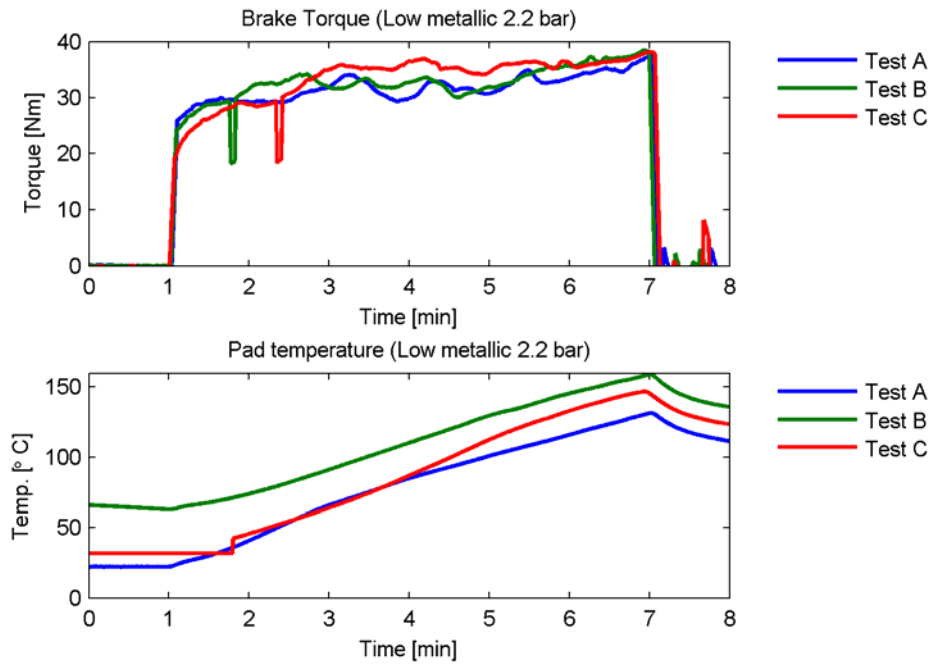


Figure 12. Brake torque and finger side pad temperature during test time for the low metallic type brake pads at 2.2 bar.

## 6.2 First test series - NAO type brake pads

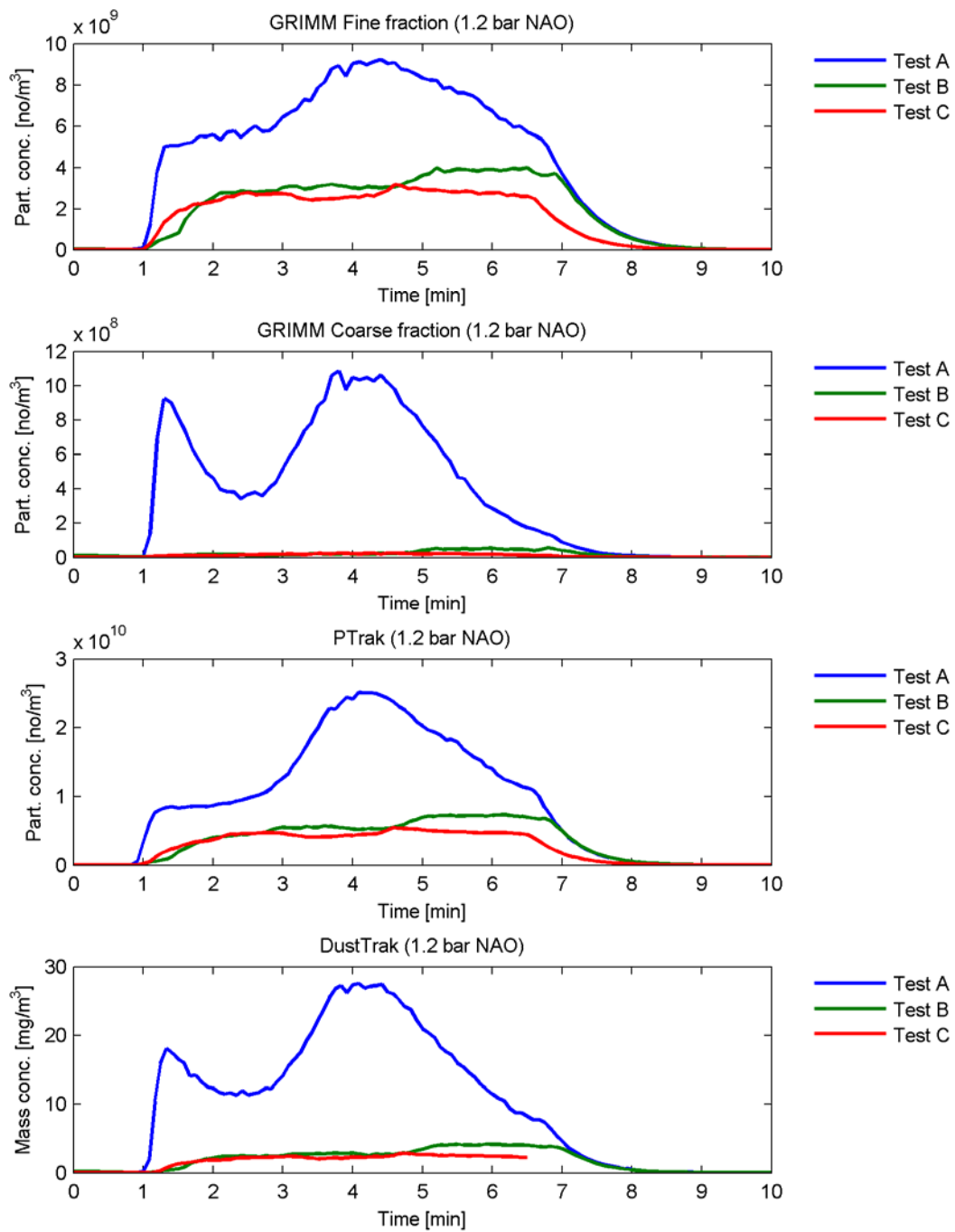


Figure 13. Particle concentrations of airborne wear particles as measured by the GRIMM instrument and the PTrak instrument, and the mass concentration as measured by the DustTrak instrument for the NAO type brake pads at 1.2 bar.

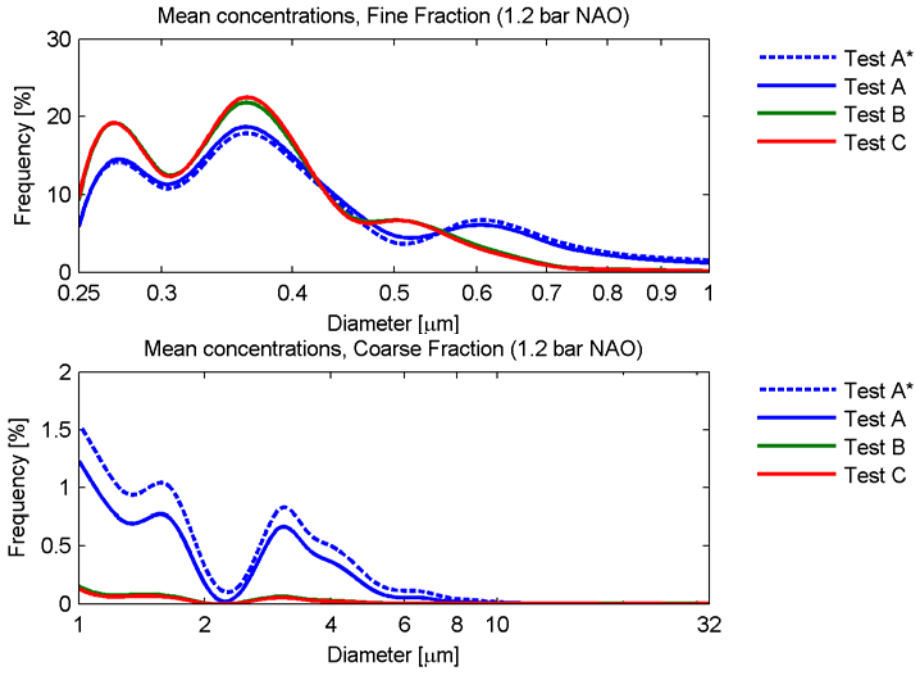


Figure 14. Mean normalized number concentration for the NAO type brake pads at 1.2 bar as measured with the GRIMM instrument. The mean is taken between 1-2.5 min and 2.5-7 min for test A\* and test A, respectively. For test B and C the mean is taken between 1-7 min.

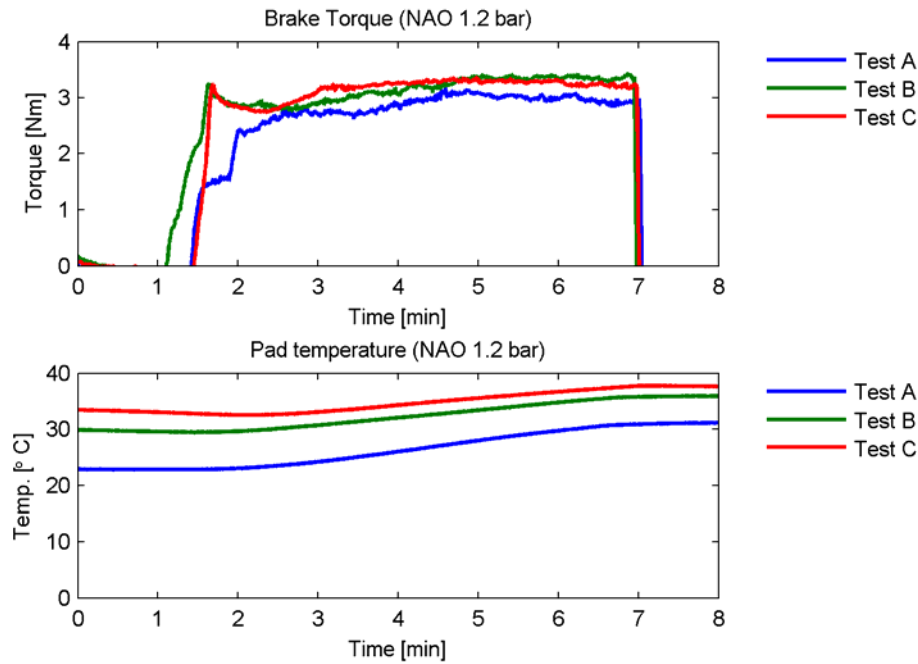


Figure 15. Brake torque and finger side pad temperature during test time for the NAO type brake pads at 1.2 bar.

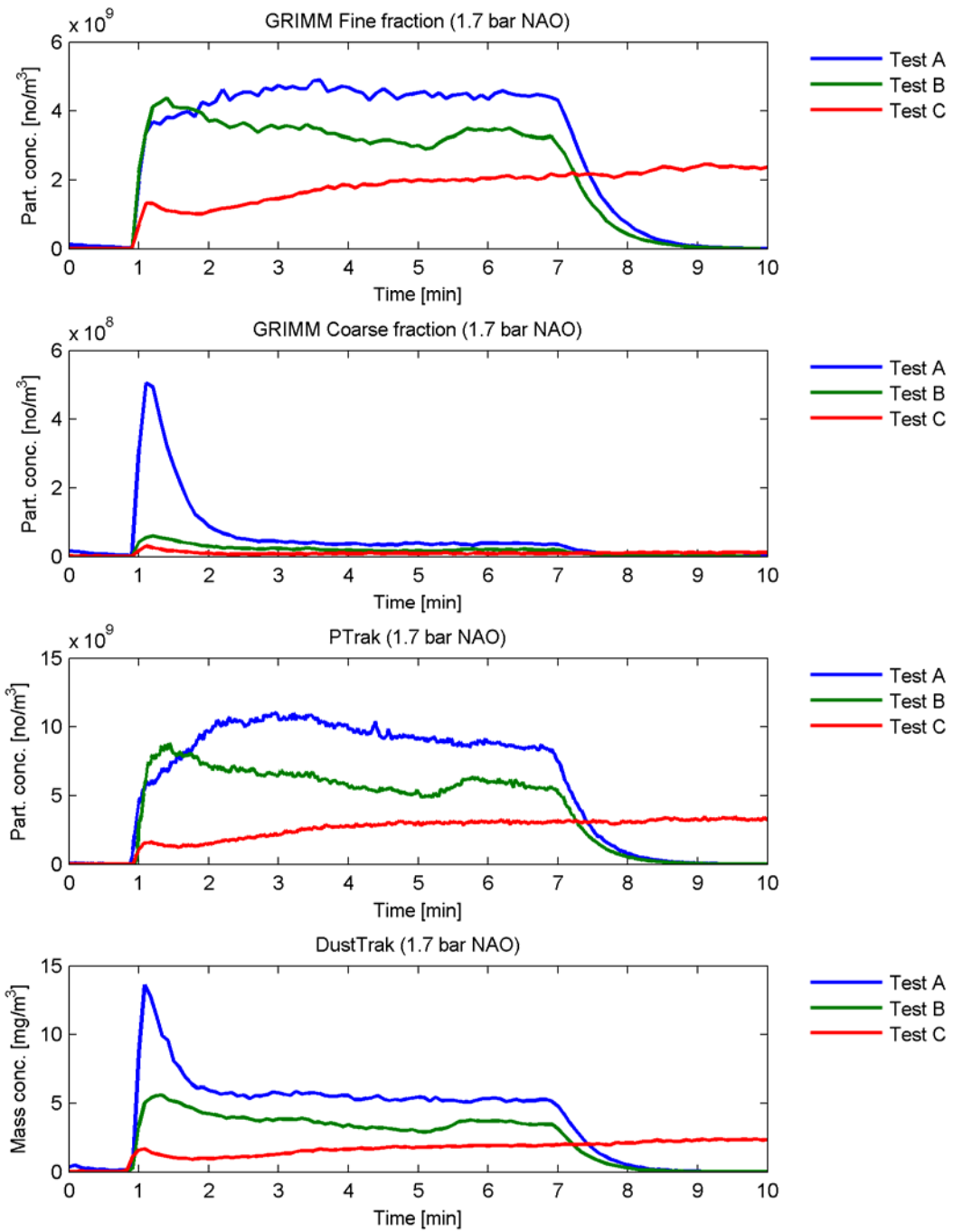


Figure 16. Particle concentrations of airborne wear particles as measured by the GRIMM instrument and the PTrak instrument, and the mass concentration as measured by the DustTrak instrument for the NAO type brake pads at 1.7 bar.

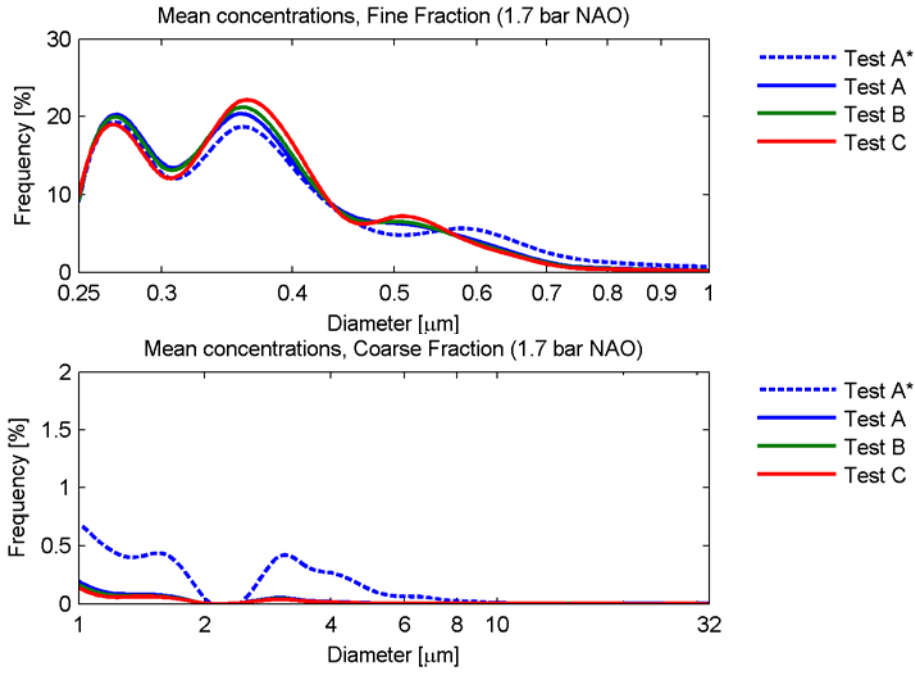


Figure 17. Mean normalized number concentration for the NAO type brake pads at 1.7 bar as measured with the GRIMM instrument. The mean is taken between 1-2.5 min and 2.5-7 min for test A\* and test A, respectively. For test B and C the mean is taken between 1-7 min.

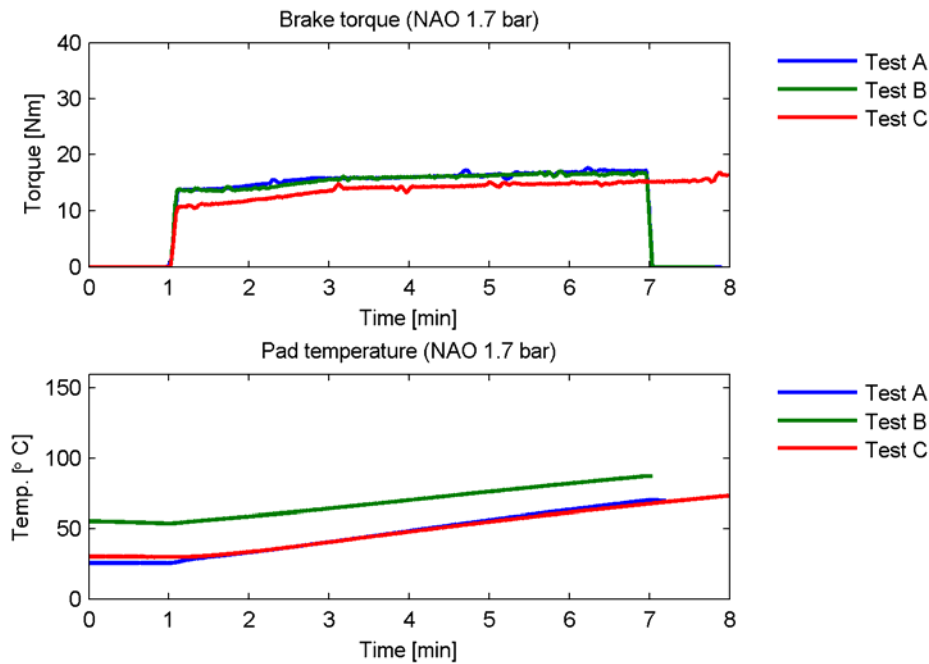


Figure 18. Brake torque and finger side pad temperature during test time for the NAO type brake pads at 1.7 bar.

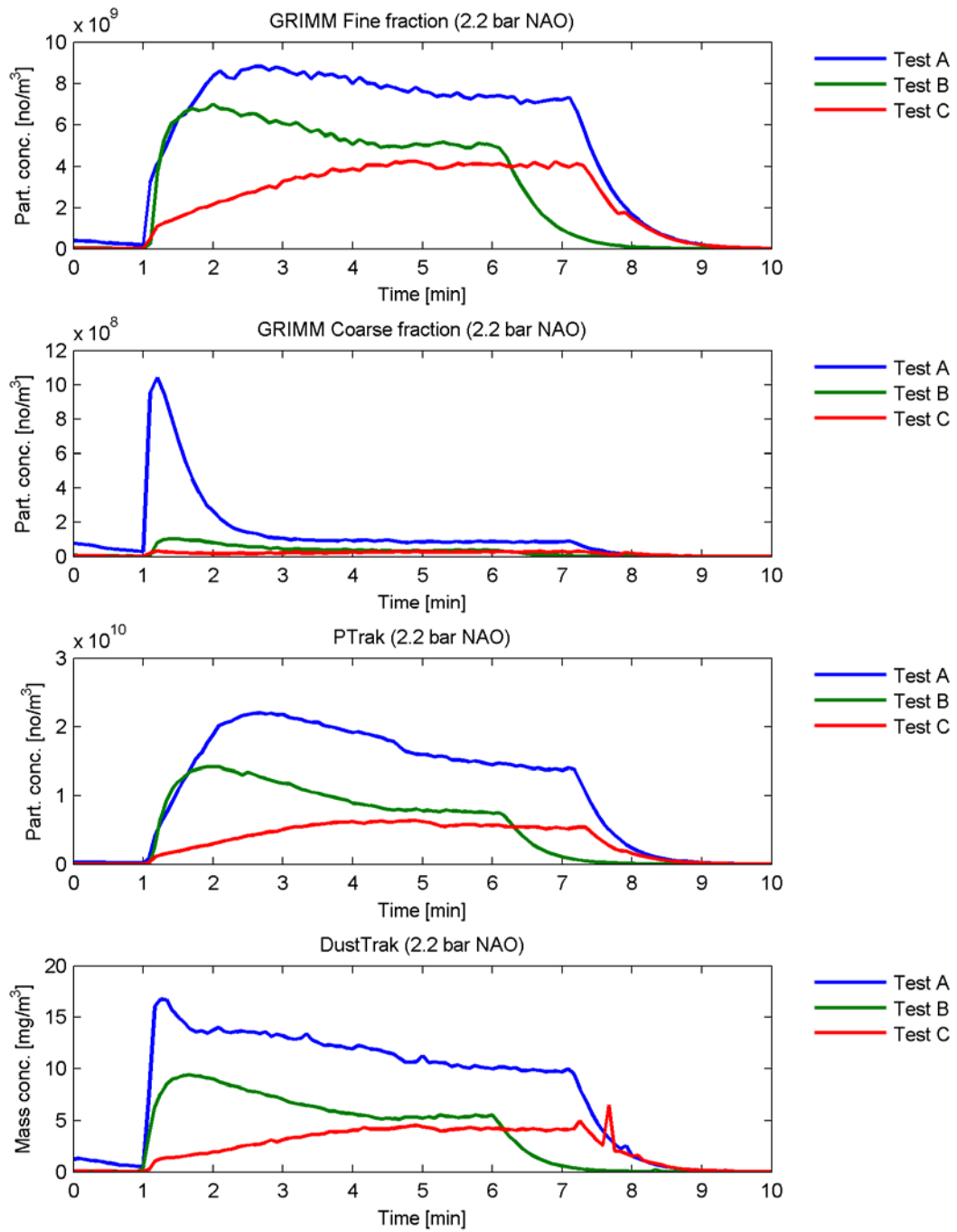


Figure 19. Particle concentrations of airborne wear particles as measured by the GRIMM instrument and the PTrak instrument, and the mass concentration as measured by the DustTrak instrument for the NAO type brake pads at 2.2 bar.

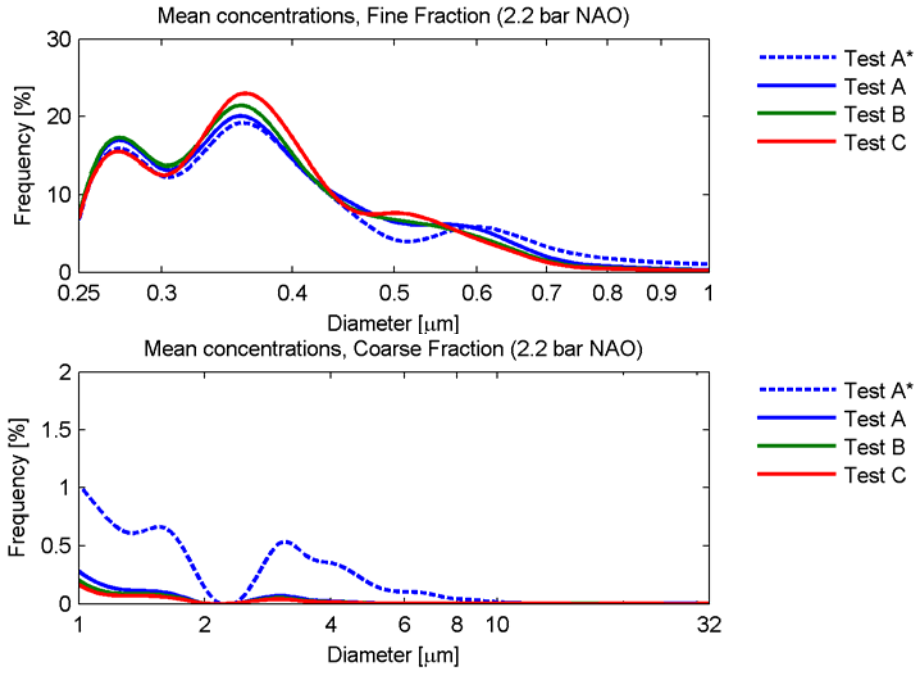


Figure 20. Mean normalized number concentration for the NAO type brake pads at 2.2 bar as measured with the GRIMM instrument. The mean is taken between 1-2.5 min and 2.5-7 min for test A\* and test A, respectively. For test B and C the mean is taken between 1-7 min.

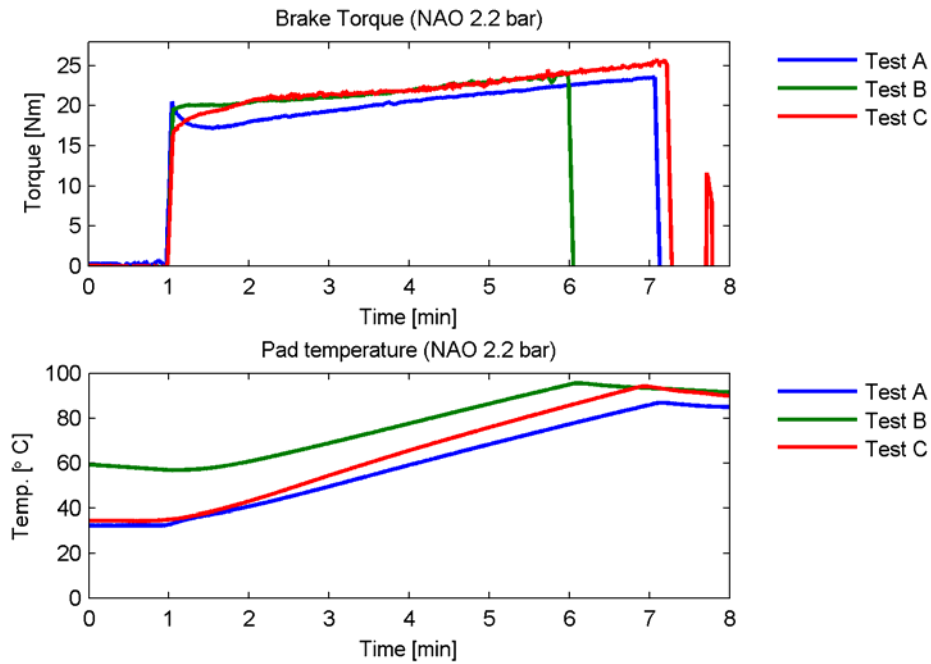


Figure 21. Brake torque and finger side pad temperature during test time for the NAO type brake pads at 2.2 bar.

### 6.3 First test series - Ceramic NAO type brake pads

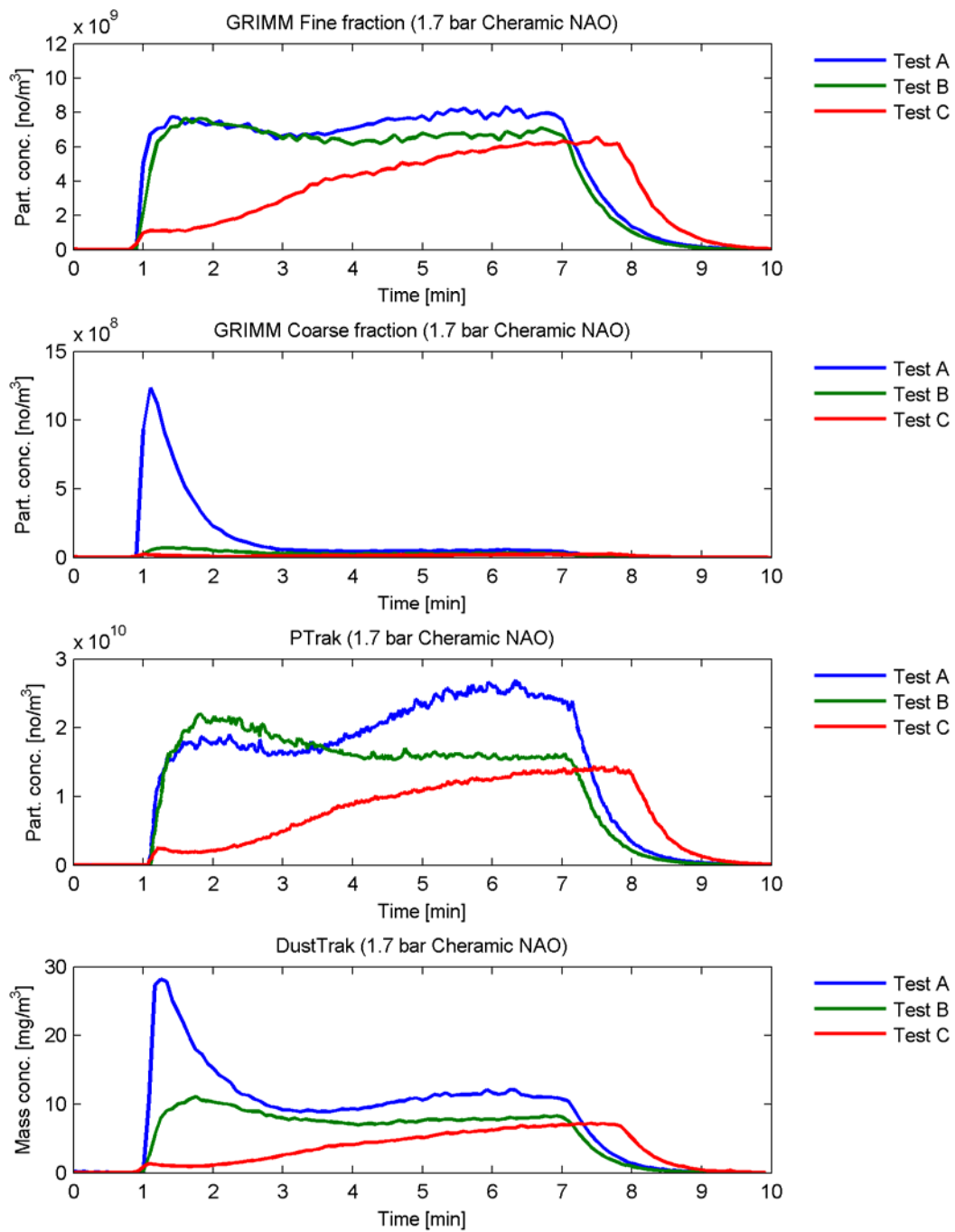


Figure 22. Particle concentrations of airborne wear particles as measured by the GRIMM instrument and the PTrak instrument, and the mass concentration as measured by the DustTrak instrument for the Ceramic NAO type brake pads at 1.7 bar.

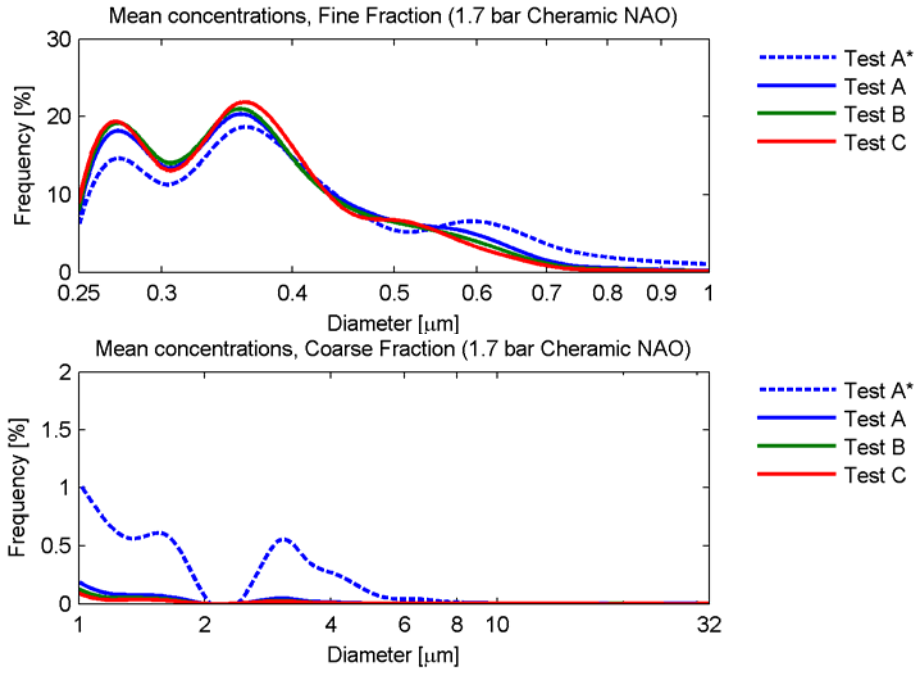


Figure 23. Mean normalized number concentration for the ceramic NAO brake pads at 1.7 bar as measured with the GRIMM instrument. The mean is taken between 1-2.5 min and 2.5-7 min for test A\* and test A, respectively. For test B and C the mean is taken between 1-7 min.

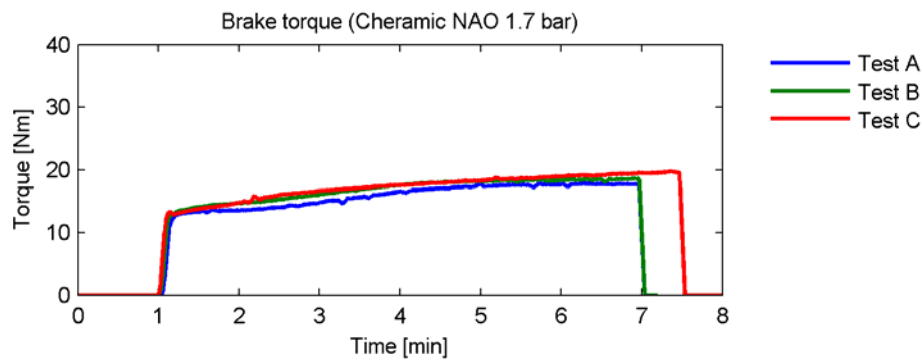


Figure 24. Brake torque during test time for the ceramic NAO type brake pads at 1.7 bar.

## 6.4 Second test series - Low metallic type brake pads

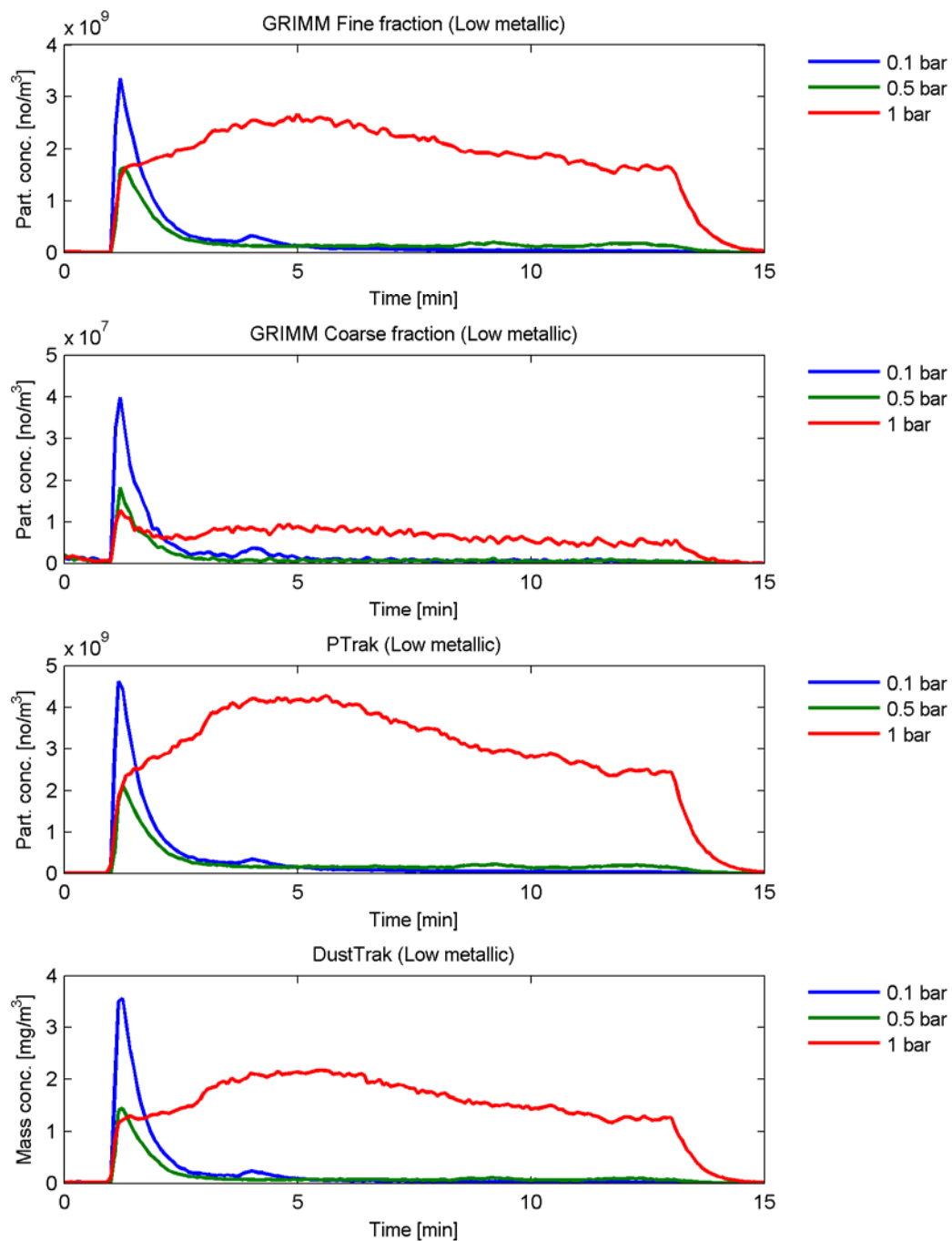


Figure 25. Particle concentrations of airborne wear particles as measured by the GRIMM instrument and the PTrak instrument, and the mass concentration as measured by the DustTrak instrument for the low metallic type brake pads at low brake cylinder pressures from 0.1 bar to 1 bar.

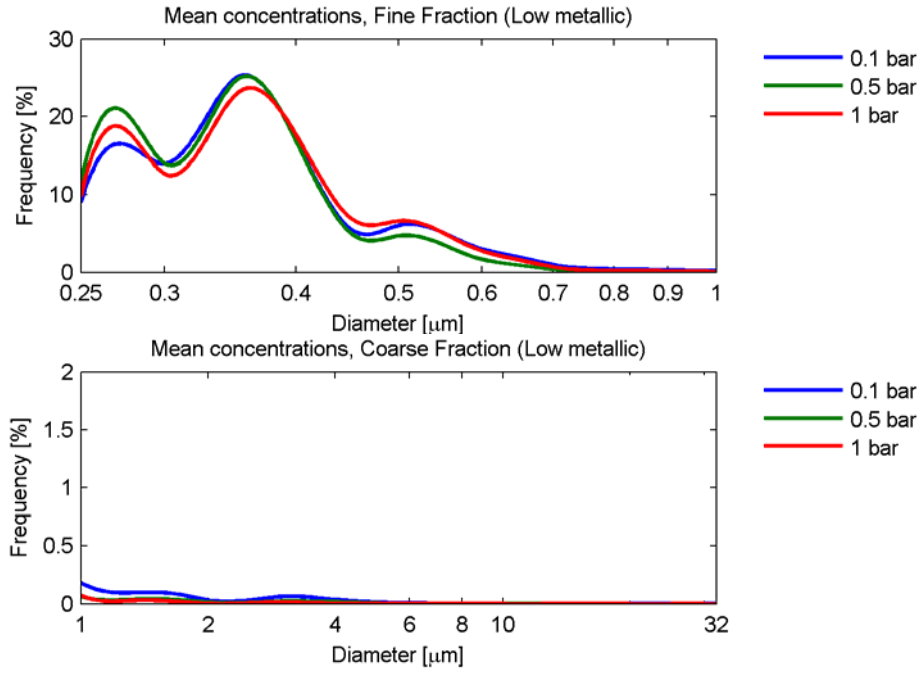


Figure 26. Mean normalized number concentration for the low metallic brake pads at low brake cylinder pressures from 0.1 bar to 1 bar as measured with the GRIMM instrument. The mean is taken between 3.5-14 min.

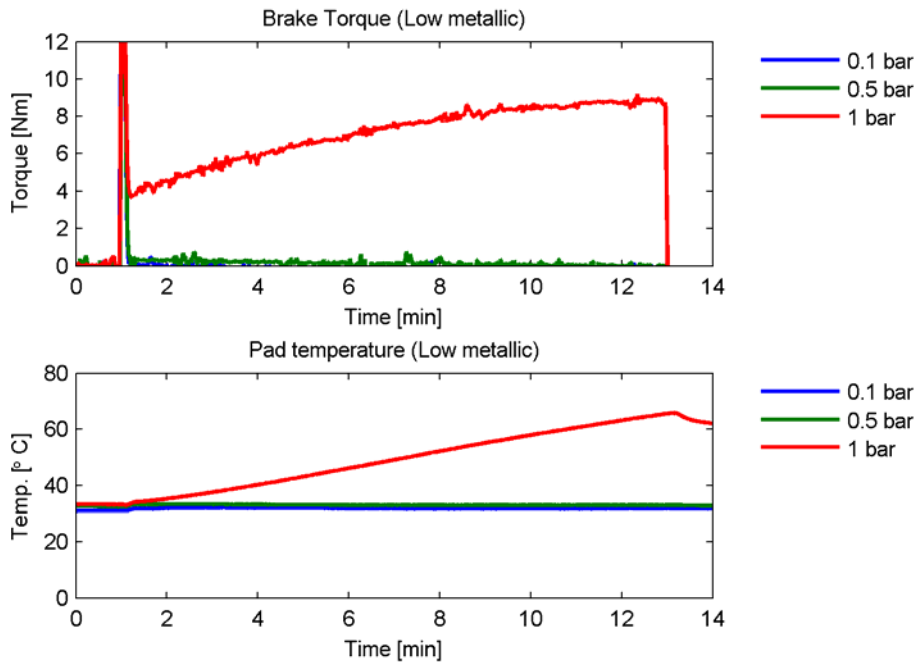


Figure 27. Brake torque and finger side pad temperature during test time for the low metallic type brake pads at low brake cylinder pressures from 0.1 bar to 1 bar.

## 6.5 Second test series - NAO type brake pads

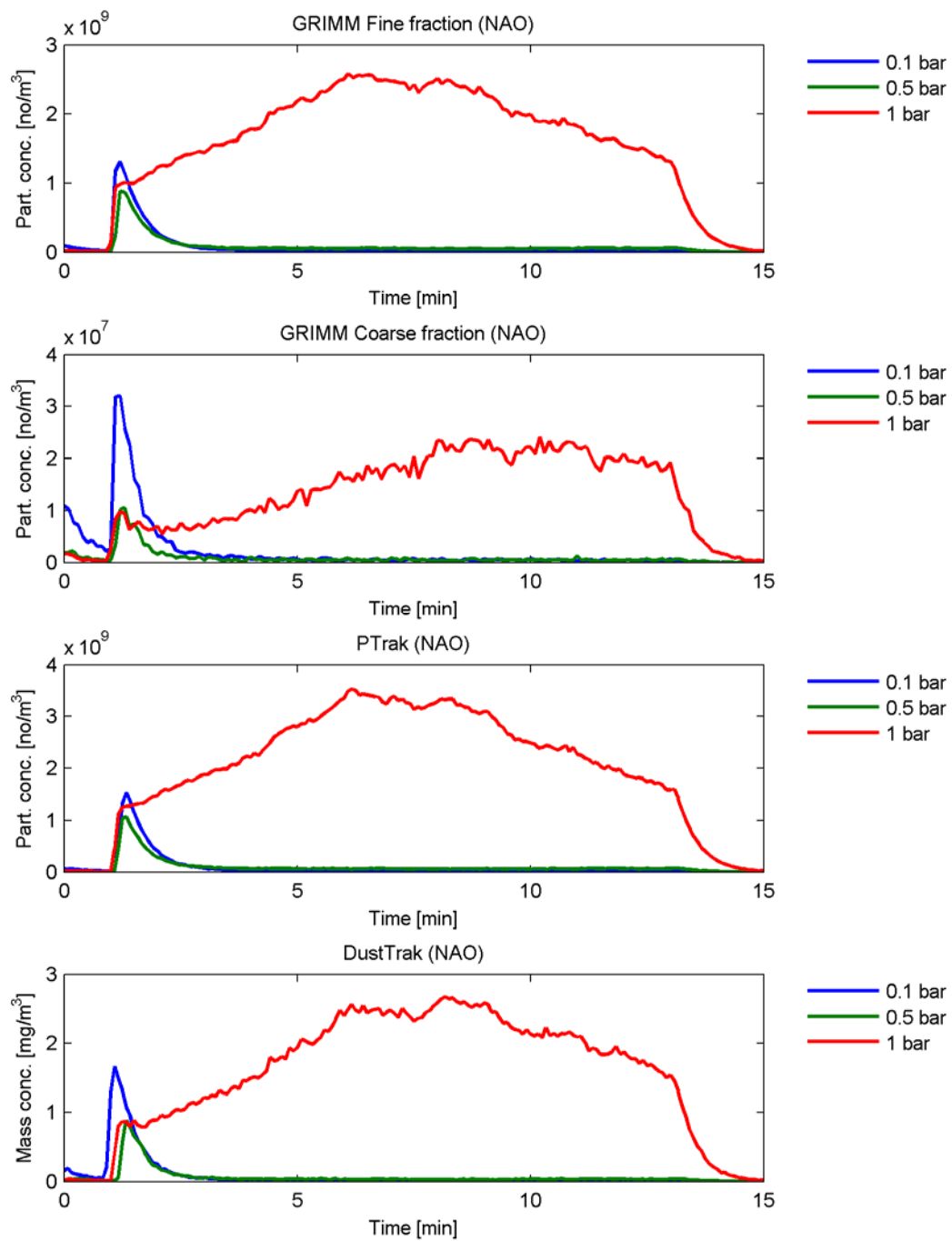


Figure 28. Particle concentrations of airborne wear particles as measured by the GRIMM instrument and the PTrak instrument, and the mass concentration as measured by the DustTrak instrument for the NAO type brake pads at low brake cylinder pressures from 0.1 bar to 1 bar.

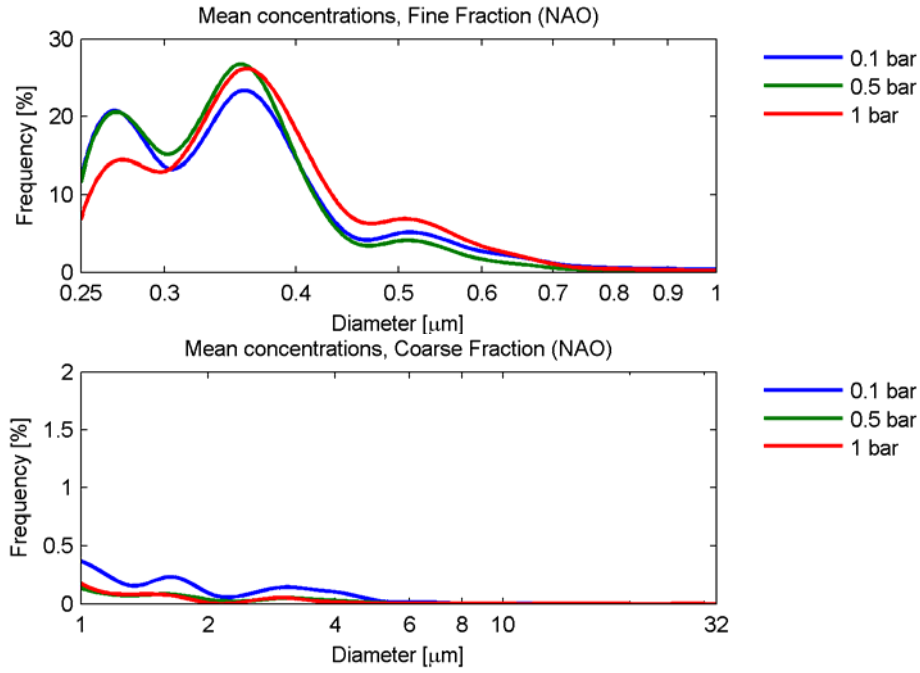


Figure 29. Mean normalized number concentration for the low metallic brake pads at low brake cylinder pressures from 0.1 bar to 1 bar as measured with the GRIMM instrument. The mean is taken between 3.5-14 min.

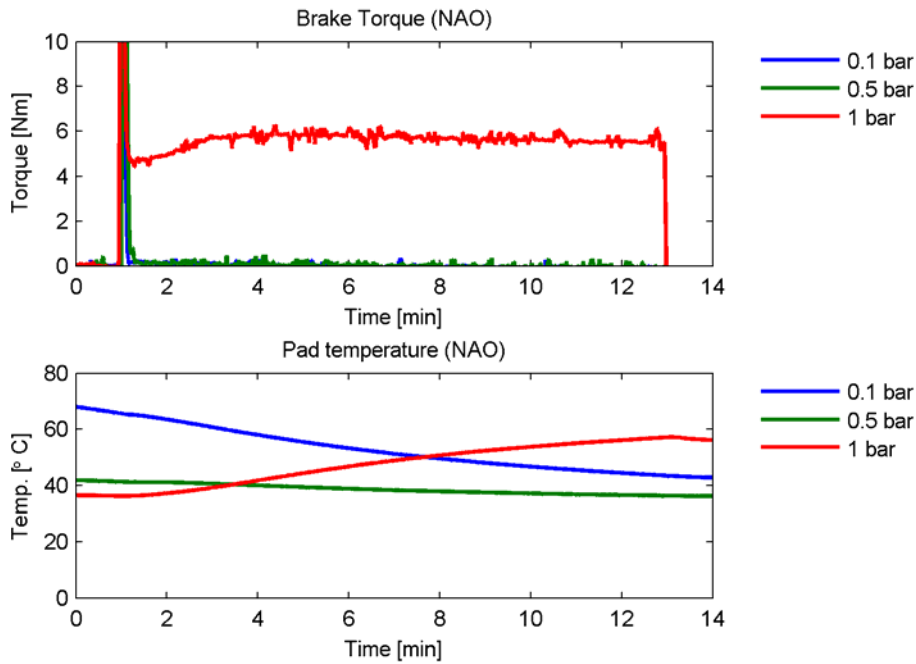


Figure 30. Brake torque and finger side pad temperature during test time for the NAO type brake pads at low brake cylinder pressures from 0.1 bar to 1 bar.

## 7 Discussion

All of the tests in the first test series have peaks in the mean particle concentration in the fine fraction around 0.28  $\mu\text{m}$  and 0.35  $\mu\text{m}$  independent of applied brake cylinder pressure and type of brake pad material used. This coincides with the results presented by Riediker et al [18] who tested different brake pad materials on different passenger cars using a box to seal of the brake from the environment. Mosleh et al [19] presented size distributions of wear particles collected on filters during pin-on-disc tests with brake materials at different testing conditions. They also noted a peak in the size distribution at 0.35  $\mu\text{m}$ , independent of contact pressure and sliding speed. Söderberg et al [17] also tested pad materials in a pin-on-disc machine and measured brake wear particles online and the particle distribution agrees with the results in this report. Moreover, Iijima et al [20] used a brake dynamometer to measure brake dust from NAO type brake pads. They noted a peak in size distribution around 0.7  $\mu\text{m}$ . Such peaks can only be found for the rotors with a rust layer here. In contrary, Sanders et al [10] conducted dynamometer and vehicle tests on pad materials, but these particle distributions do not confirm the results in this report.

In the beginning for all tests A in the first test series, a distinct peak in particle concentration in the coarse fraction as measured by the Grimm can be observed. This peak is up to a factor 5 larger than the number of airborne wear particles generated after this peak. The mean particle distribution for test A after this peak is similar to the distribution for test B and C, which were conducted without an oxide layer. Furthermore, in the tests with an applied brake cylinder pressure of 1.2 and 1.7 bar the brake torque started at a constant level for about 20 seconds and thereafter increased to reach a higher steady level. In the tests with 2.2 bar applied brake cylinder pressure the brake torque almost directly increased towards a steady level. One possible interpretation of these results is that this is the time for the oxide layer removal and that the particle measurements together with the torque measurement can be used as an indicator of oxide removal. Further tests are necessary to evaluate this phenomenon.

The ceramic NAO pads generate the highest mean concentration of airborne particles at 1.7 bar brake cylinder pressure. The low metallic pads is about the same level as the NAO pads after the oxide layer removal but is up to a factor two higher during the removal. For most of the tests the mean particle concentration is higher for the low metallic pads than for the NAO pads. This may be explained by that the low metallic pads are more aggressive than the NAO pads. These results are in line with the results from pin-on-disc tests Söderberg et al [16] were the low metallic pad material pins against cast iron material discs generated more wear and also more airborne particles compared to the NAO pad cast iron combination. These two results show a promising capability with the test set up to rank different pad to rotor material combinations ability to generate airborne wear particles during different operating conditions. Note that the concentration is lower for test C which started from room temperature than test B which

was conducted directly after test A. One interpretation of this is that more airborne particle is generated when the temperature in the contact is higher. The results are in line with the results from field tests Olofsson et al [21]. Furthermore, Sanders et al [10] conclude that the wear rates are material dependent with 3-4 times higher emissions observed from the low metallic type of brake pads and that the particle concentration increases with increasing temperature. To verify this temperature dependence more tests have to be conducted.

Additionally, for the NAO and the low metallic type brake pads there is a maximum in the particle concentration for the coarse fraction around 3  $\mu\text{m}$  for the mean particle distributions taken between 1-2.5 min. This peak gets smaller after 2.5 minutes in all tests, except for the NAO type brake pads at 1.2 bar cylinder pressure. One interpretation of this is that the oxide layer is not worn off during the test, i.e. 1.2 bar brake cylinder pressure may not be enough to clean the rotor from a rust layer. To investigate the sliding distance needed to clean the rotor from an oxide layer at different low pressure levels this test stand can be used if further tests show that particle and torque measurements can be used as indicators of oxide removal. It would also be of interest to prepare the rotor with road salt and water before or during the tests.

Note that measurable levels of particle concentration can be registered even at low brake cylinder pressures which indicate that the pads are in contact with the rotor. This is interesting because some brake systems may require the pads to be frequently in low pressure contact to keep the contact surface between the pad and disc clean. In order to decrease the number of airborne wear particles generated it is interesting to decrease the contact time between the pads and rotor even at low pressures. But to ensure robust braking, increased knowledge about the rotor cleaning is needed. For both the NAO and low metallic type of brake pads the measured brake torque (Figure 27 and Figure 30), after the initial braking for 0.1 and 0.5 bar is about zero. The measured torque is in the interval of accuracy for the sensor. It would be interesting to further investigate the brake torque with higher accuracy of the torque measurement at low pressures, also known as drag torque, to see how much energy that is used in this cleaning function. Note the large difference in particle concentration and brake torque for 0.5 and 1 bar. One interpretation of this is that a cylinder pressure between these levels is needed to keep the pads in contact with the rotor after the initial braking load. Furthermore, the mean normalized particle concentration (Figure 26 and Figure 29) for both the NAO and low metallic type of brake pads has peaks around 0.28, 0.35 and 0.5  $\mu\text{m}$  which is similar to the result from the first test series.

Most of the mass concentrations curves as measured by the DustTrak instrument resemble the shape of the particles concentrations curves as measured by the GRIMM instrument and the shape of the particle concentration curves as measured by the PTrak

instrument agree with the shape of the particle concentration curve as measured by the GRIMM instrument. For the tests with an oxide layer the mass and particle concentrations as measured by the DustTrak and the PTrak doesn't agree with the GRIMM in the beginning. Note that the PTrak counts particles from 0.02  $\mu\text{m}$ , while the lower limit for the GRIMM is 0.25  $\mu\text{m}$ , i.e. the PTrak register a higher particle concentration, if airborne wear particles with a particle size smaller than 0.25  $\mu\text{m}$  are generated. Also note that the DustTrak instrument measures mass concentration so small particles sizes will give a small contribution to the mass concentration level and therefore it can be compared with the shape of the coarse particle concentration curve measured by the GRIMM. In the first and the second test series most of the airborne particles generated is in the fine fraction. Therefore it would be interesting to measure particle concentration in the ultra fine fraction in size intervals to study the particle distribution there.

Furthermore, during braking, there is wear to both the rotor and the pads. An estimation of how many of the wear particles originate from the rotor and the pads can be done by analyzing the filters. The friction between the rotor and pads is one important factor for the brake behaviour and it is therefore interesting to estimate the coefficient of friction. For calculation of an apparent coefficient of friction, the effective radius (i.e., the radial location at which a single force may be placed to create the same torque on the brakes) between the rotor and the pads must be known. Antanaitis and Sanford [22] used a piezoelectric pressure instrument, TekSkan, to measure the contact area and pressure distribution in the rotor to pads contact, and calculated the effective radius. This instrument can be used before and after testing to estimate the effective radius and, thereafter, calculate an apparent coefficient of friction.

Both test series were conducted under stationary load conditions. It would be of interest to extend the test stand to more realistic (transient) braking events. This can be done by controlling the pressure from the pneumatic system and the rotational speed of the motor to simulate typical braking events. Also, the validity of this test stand has to be verified by comparison with field tests.

## 8 Conclusions

Promising results from a first test series indicate that this test stand can be used to study oxide layer removal from the rotor. The results are also promising for the ability to rank the number and size distribution from different pad rotor material combinations. The results from the second test series shows that a measurable amount of airborne particles can be generated even at low contact pressure levels.

## 9 References

- [1] Katsouyanni K, Touloumi G, Samoli E, Gryparis A, Le Tertre A, Monopolis Y, Rossi G, Zmirou D. Confounding and effect modification in the short-term effects of ambient particles on total mortality: results from 29 European cities within the APHEA2 project. *Epidemiology* 2001; **12(5)**: 521-531.
- [2] Samet JM, Dominici F, Curriero FC, Coursac I, Zeger SL. Fine particulate air pollution and mortality in 20 U.S. cities 1987-1994. *N Engl J Med* 2000; **343(24)**: 1742-1749.
- [3] Pope CA, Burnett RT, Thun MJ, Calle EE, Krewski D, Ito K, Thurston GD. Lung cancer, cardiopulmonary mortality, and long-term exposure to fine particulate air pollution. *JAMA* 2002; **287**: 1132-1141.
- [4] X. Querol et al. Speciation and origin of PM10 and PM2.5 in selected European cities. *Atmospheric Environment* 2004; **38**: 6547–6555.
- [5] Mahmoud Abu-Allaban, John A. Gillies, Alan W. Gertler, Russ Clayton, David Proffitt. Tailpipe, resuspended road dust, and brake-wear emission factors from on-road vehicles. *Atmospheric Environment* 2003; **37**: 5283–5293.
- [6] Seaton A, Cherrie J, Dennekamp M, Donaldson K, Hurley J, Tran C. The London underground: dust and hazards to health. *Occup Environ Med* 2005; **62(6)**: 355–362.
- [7] Branis M. The contributions of ambient sources to particle pollution in spaces and trains of the Prague underground transport system. *Atmospheric Environment* 2006; **40(2)**: 348–356.
- [8] Abu-Allaban M, Gillies, JA, Gertler AW, Clayton R, Proffitt D. Tailpipe, resuspended road dust, and brake-wear emission factors from on-road vehicles. *Atmospheric Environment* 2003; **37(37)**: 5283–5293.
- [9] Weckwerth G. Verification of traffic-emitted aerosol components in the ambient air of Cologne (Germany). *Atmospheric Environment* 2001; **35(32)**: 5525–5536.

- [10] Sanders PG, Xu N, Dalka TM, Marico M. Airborne brake wear debris: size distributions, composition of dynamometer and vehicle test. *Environmental Science and Technology* 2003; **37(18)**: 4060–4069.
- [11] Loug G, Schaur JJ, Soopark J, Shafer M, Deminter J, Weinstein J. Emission of metals associated with motor vehicle roadways. *Environmental Science and Technology* 2005; **39(3)**: 826–836.
- [12] Blau PJ, Meyer III HM. Characteristics of wear particles produced during friction tests of conventional and unconventional disc brakes materials. *Wear* 2003; **255(7-12)**: 1261–1269.
- [13] Garg DG, Cadle SH, Mulawa PA, Groblicki PJ. Brake wear particle matter emission. *Environmental Science and Technology* 2000; **43(21)**: 4463–4469.
- [14] Olofsson U, Olander L. On the identification of wear modes and transitions using airborne wear particles generated from sliding steel-on-steel contact. Submitted for publication (2007).
- [15] Olofsson U, Olander L, Jansson A. Airborne particles from two different steel combinations during sliding contact. To be submitted (2008).
- [16] Söderberg A, Wahlström J, Olander L, Jansson A, Olofsson U. On Airborne Wear Particles Emissions of Commercial Disc Brake Materials – A Pin on Disc Simulation. Technical report (2008).
- [17] Wahlström J, Söderberg A, Olander L, Olofsson U. A disc brake test stand for measurement of airborne wear particles. Presented at the 13th Nordic Symposium on Tribology.
- [18] Riediker M, Gasser M, Perrenoud A, Gehr P, Rothen-Rutishauser B. A system to test the toxicity of brake wear particles presented at the 12th ETH-Conference on Combustion Generated Nanoparticles.
- [19] Mosleh M, Blau PJ, Dumitrescu D. Characteristics and morphology of wear particles from laboratory testing of disc brake materials. *Wear* 2004; **256(11-12)**: 1128-1134.

[20] Iijima A, Sato K, Yano K, Kato M, Kozawa K, Furuta N. Emission factor for antimony in brake abrasion dust as one of the major atmospheric antimony sources. *Environmental Science and Technology* 2008; **42(8)**: 2937-2942.

[21] Olofsson U, Wahlström J, Olander L, Jansson A. On Airborne Wear Particles Emissions of Commercial Disc Brake Materials – Field test in Stockholm. Technical report (2008).

[22] Antanaitis D, Sanford J. The effect of racetrack/high energy driving on brake caliper performance. *SAE Brake Technology* 2006.